ANCIENT DNA

Paleogenomics and habitat modeling reveal temperate Eurasian origins of woolly rhinoceroses

Xiao-Le Lei (雷晓乐)[1,2,3]†, Jiaoyang Ruan (阮骄杨)[4,5]†, Xueyuan Liang (梁雪原)[1], Raquel Teixeira[6,7], Jiangyue Zhang (张江月)[1], Alexandre Gilardet[6,8], Xu Zhou (周旭)[1], Yu Han (韩雨)[1], Zhihan Zhao (赵致晗)[1], Hai-Yan Yue (岳海岩)[1], Maxim Kozlikin[9], Sergey Vasiliev[9], Stanislav Medvedev[10], Sergei Kruskop[11], Song Xing (邢松)[12], Ting Wang (王婷)[13], Vera Basova[14], Lijuan Ma (马丽娟)[15], Bohua Shi (史博华)[16], Qingfeng Shao (邵庆丰)[17], Katerina Douka[18,19], Michael Shunkov[9], Alexandra Buzhilova[10], Love Dalén[6,8,20], He Yu (遇赫)[1,2]*

The woolly rhinoceros was a prominent Ice Age megafaunal species, and there is limited knowledge regarding its origin and responses to past glacial cycles. We sequenced 29 mitochondrial and 14 nuclear genomes from Pleistocene specimens across Eurasia and modeled the species' habitats over the past 500,000 years. Our results suggest that its maternal genetic diversity mainly evolved in temperate Eurasia around 460 thousand to 420 thousand years ago during a prolonged glacial-interglacial transition. We found that a ~170-thousand-year-old East Asian individual was ancestral to all later populations, indicating East Asia as one possible origin of Late Pleistocene ancestry. We also identified the Altai region as a major climatic refugium. These findings highlight the crucial role of temperate Eurasia in the evolution of woolly rhinoceroses and the diversification of cold-adapted megafauna.

The woolly rhinoceros (*Coelodonta antiquitatis*) was an iconic cold-adapted species that dominated northern Eurasia during the Late Pleistocene, from ~130 thousand to 11 thousand years ago (ka) (*1*–*3*). The *Coelodonta* lineage is believed to have evolved its adaptations to cold climate in high-altitude regions following an "out-of-Tibet" evolutionary pathway (*4*), with the earliest *Coelodonta* fossil found on the Tibetan Plateau dated to 3.7 million years ago (*5*). Likely derived from *C. tologoijensis* (*6*) in East Eurasia, the earliest known fossil of a woolly rhinoceros was found in Central Europe and dated to ~450 ka (*7*, *8*), yet the details of how this species dispersed and colonized Eurasia remain elusive. *Coelodonta* went extinct near the onset of the Holocene (11 ka to present), with the last fossil evidence from ~14 ka (*2*) and sediment DNA indicating that it may have survived until at least ~9.8 ka (*9*). The causes of its extinction remain debated and have been attributed to various climatic and anthropogenic factors (*10*–*12*). Although the species survived through multiple glacial-interglacial cycles in the Middle Pleistocene (700 to 130 ka) and Late Pleistocene, it remains unclear whether these extreme climatic oscillations led to its population substructuring or played a role in its population decline.

Ancient genomic studies have resolved the phylogenetic relationship of the woolly rhinoceros with extant and extinct rhinoceroses (*13*) and reconstructed its demographic history (*11*, *14*). However, the only three available nuclear genomes derive exclusively from Late Pleistocene Northeast Siberia, leaving most of the species' former distribution, particularly in mid-latitude Eurasia, genetically underrepresented (*11*, *13*, *14*). Mitochondrial genomes from East Asia (*15*) and Europe (*16*) revealed genetic diversities that had been previously undiscovered among Northeast Siberian individuals but lacked the resolution to reconstruct the population structure of the species. Previous studies on another representative cold-adapted species, the woolly mammoth, identified high-latitude Siberia as its primary center of genetic diversity (*17*, *18*). However, the woolly rhinoceros developed cold adaptation through distinct evolutionary strategies (*4*) and occupied more southerly habitats in East Asia than most other members of the *Mammuthus-Coelodonta* complex (*1*). Therefore, whether it showed similar population dynamics to the woolly mammoth, with genetic diversity emerging in high-latitude areas (*17*, *18*), is also subject to discussion.

To address these questions, we screened 183 woolly rhinoceros fossils from across Eurasia (data S1 and S2) and successfully reconstructed 29 mitochondrial genome sequences (8.2× to 468.7×) and 14 nuclear genomes (0.5× to 14.1×) from East Asia, the Altai, and Europe (Fig. 1A and data S1). These genomes were sequenced on both the NovaSeq (Illumina) and MGISEQ (BGI) platforms, and there is no evidence to suggest that combining data from these two sequencing platforms introduces bias or affects downstream analyses (fig. S1). Using a combination of direct radiocarbon dating (data S3), U-series dating (data S4), stratigraphic dating (data S5), and molecular dating (data S6) strategies, 1 fossil was dated to Marine Isotopic Stage (MIS) 7 (243 to 191 ka), 2 to MIS 6 (191 to 130 ka), 12 to MIS 5 (130 to 71 ka), 9 to MIS 3 (57 to 29 ka), and 5 to MIS 2 (29 to 11 ka) (Fig. 1B and data S1). We assessed the discrepancies among different dating methods (fig. S2, data S7, and supplementary materials section "Comparison of molecular dating estimates with independent dating results") and concluded that molecular dating provides a relatively reliable temporal reference for samples that lack both finite radiocarbon dates and stratigraphic age constraints. Consequently, any dating uncertainties are expected to have a negligible impact on subsequent genetic analyses. These newly sequenced genomes were analyzed alongside 20 previously published mitochondrial genomes and two nuclear genomes of woolly rhinoceros (data S8), one mitochondrial and three nuclear genomes of Sumatran rhinoceros (*Dicerorhinus sumatrensis*), and one mitochondrial and nuclear genome of Merck's rhinoceros (*Stephanorhinus kirchbergensis*) (*11*, *13*, *15*, *16*).

To evaluate the influence of climate-driven habitat dynamics on the population history and genetic structure of the woolly rhinoceros, we developed a habitat-suitability model based on the Mahalanobis distance framework (*19*). The model integrates 1153 fossil occurrences (data S9) with four key climatic predictors—annual mean temperature, minimum temperature, precipitation, and net primary productivity—that together capture the species' thermal tolerance, water availability, and food-resource potential (*20*) (figs. S3 and S4

[1]State Key Laboratory of Gene Function and Modulation Research, School of Life Sciences, Peking University, Beijing, China. [2]Institute of Ecology, Peking University, Beijing, China. [3]Peking University-Tsinghua University-National Institute of Biological Sciences Joint Graduate Program, School of Life Sciences, Tsinghua University, Beijing, China. [4]State Key Laboratory of Lithospheric and Environmental Coevolution, Institute of Geology and Geophysics, Chinese Academy of Sciences, Beijing, China. [5]Center for Climate Physics, Institute for Basic Science, Busan, Republic of Korea. [6]Centre for Palaeogenetics, Stockholm, Sweden. [7]Department of Biology, Faculty of Sciences of the University of Lisbon, Lisbon, Portugal. [8]Department of Zoology, Stockholm University, Stockholm, Sweden. [9]Institute of Archeology and Ethnography of the Siberian Branch of the RAS, Novosibirsk, Russia. [10]Research Institute and Museum of Anthropology, Lomonosov Moscow State University, Moscow, Russia. [11]Zoological Museum of Lomonosov Moscow State University, Moscow, Russia. [12]Institute of Vertebrate Paleontology and Paleoanthropology, Beijing, China. [13]Natural History Museum of China, Beijing, China. [14]Vernadsky State Geological Museum, Moscow, Russia. [15]Quaternary Paleontology Fossil Museum of Qinggang, Suihua, China. [16]Qinggang County Cultural and Tourism Bureau, Suihua, China. [17]School of Geography, Nanjing Normal University, Nanjing, China. [18]Department of Evolutionary Anthropology, Faculty of Life Sciences, University of Vienna, Vienna, Austria. [19]Human Evolution and Archaeological Science (HEAS) Research Cluster, Vienna, Austria. [20]Department of Bioinformatics and Genetics, Swedish Museum of Natural History, Stockholm, Sweden. ***Corresponding author. Email: yuhe@pku.edu.cn** †These authors contributed equally to this work.

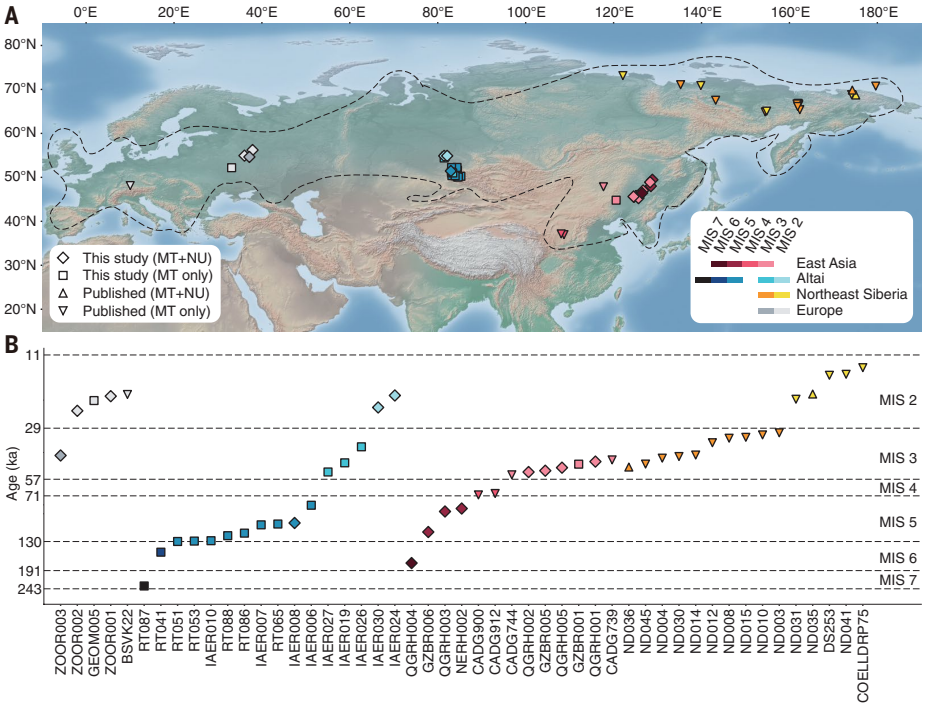

Fig. 1. Locations and ages of newly reported samples. (**A**) Geographic locations of woolly rhinoceroses. Colors represent the geographic regions of the samples, and color gradients represent their temporal periods. Marker types differentiate samples newly generated in this study, previously published samples, samples with mitochondrial genomes only (MT only), and samples with both mitochondrial and nuclear genome data (MT+NU). (**B**) Ages of woolly rhinoceroses. The marker types are the same as in (A). The *y* axis represents ages on a logarithmic scale for better visualization.

and data S10). Derived from time-varying Pleistocene climate and biome simulations (*21*, *22*), these variables were reconstructed over the past 500 thousand years (kyr) at a 1-kyr temporal resolution and 0.5° spatial resolution, spanning the full range of fossil evidence. This framework allowed us to track spatiotemporal changes in suitable habitat, quantify temporal variation in habitat area and fragmentation, and evaluate the robustness of the inferred habitat dynamics (figs. S5 to S8 and movie S1).

Mitochondrial diversification tracing back to MIS 11

With the comprehensive mitochondrial genome dataset, we assessed the phylogenetic relationship among woolly rhinoceroses across Eurasia and identified four haplogroups (named clades 1 to 4) (Fig. 2A and fig. S9). The time to the most recent common ancestor of all woolly rhinoceroses' mitochondrial genomes was estimated to be 464 ka (95% highest posterior density: 527 to 409 ka; Fig. 2A), close to the age of the earliest known fossil of *C. antiquitatis* (*7*). The four clades diverged between 464 and 417 ka (Fig. 2A), overlapping with a prolonged climatic transition from MIS 12 (478 to 424 ka) to MIS 11 (424 to 374 ka) that was marked by increased habitat fragmentation and contraction across Eurasia (Fig. 3, A to C, and fig. S7).

According to haplogroup frequencies, clades 1 and 2, first reported in Northeast Siberian individuals (*11*), were mainly found in East Asia and Northeast Siberia, whereas clades 3 and 4 were mainly found in Altai and Europe (Fig. 2B), indicating a genetic differentiation between East and West Eurasian populations. The fixation index (F_{ST}) among different regions also suggests a close relation between European and Altai woolly rhinoceroses (data S11). The presence of all four clades in the Altai region underscores an important role of the Central–East Asia transition zone in the maternal evolution of woolly rhinoceroses. This is supported by habitat-suitability model results showing that suitable habitats in this region persisted throughout glacial-interglacial cycles (Fig. 3F). The nucleotide diversity in the Northeast Siberian population was the lowest among all studied regions (data S12). This suggests that, unlike the woolly mammoth (*17*), the genetic diversity of woolly rhinoceros more likely emerged in warmer, lower-latitude regions, consistent with its southward distribution during the cooling periods (*10*, *23*).

Taking these findings together with range-wide sampling, we detected an East-West differentiation in the maternal ancestry of woolly rhinoceroses and revealed a higher genetic diversity in mid-latitude Eurasia than in high-latitude regions. With home ranges <100 km^2, the rhinoceroses (*24*, *25*) are generally considered much less mobile than elephants, which could migrate 1000 km in an individual's lifetime (*26*–*28*). Lower mobility would be expected to promote stronger phylogeographic structure. On the contrary, the phylogeographic substructure among woolly rhinoceroses (Fig. 2) was not as strong as that observed in woolly mammoths (*29*). Similarly, extant rhinoceroses also showed relatively weak mitochondrial phylogeographic structure (figs. S10 and S11) (*30*, *31*), whereas substantial substructuring was observed in African forest and savanna elephants, despite their high mobility (*32*).

One possible explanation is that compared with the solitary lifestyle of the Rhinocerotidae (*33*, *34*), the matrilineal social structure of the Elephantidae (*35*, *36*) may more readily give rise to a distinct phylogeographic structure in mitochondrial DNA, as females tend to be more philopatric (*37*), and result in more localized mitochondrial haplogroups. In addition, habitat-suitability modeling suggests that woolly rhinoceroses may have experienced repeated range contractions and reexpansions over the past ~500 kyr (movie S1), potentially eroding mitochondrial phylogeographic structure. Genetic data covering broader geographic and temporal ranges will be essential to further validate these different hypotheses.

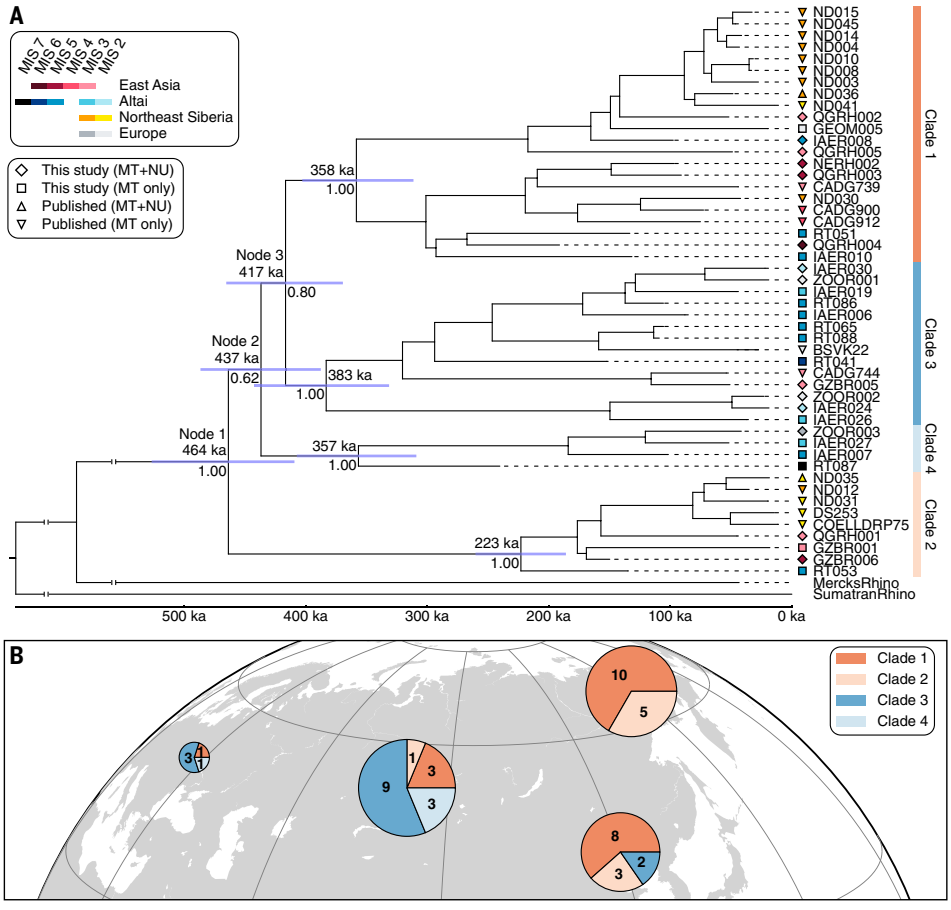

Fig. 2. Mitochondrial phylogeny and geographic structure among woolly rhinoceroses. (**A**) Bayesian phylogeny of newly reported and published individuals using mitochondrial genomes. Numbers above and below the nodes show the median ages and posterior probabilities, respectively, and the bars show the 95% highest posterior density of estimated ages. The color and shape of each sample show the region and age corresponding to Fig. 1. The colored bars indicate four different haplogroups. (**B**) Frequencies of each haplogroup across different regions. Colors represent different haplogroups. Pie-chart sizes are scaled according to the number of mitochondrial genomes in each region, and the numbers labeled in each segment represent the number of mitochondrial genomes belonging to each clade.

Temperate Eurasian origin of Late Pleistocene woolly rhinoceroses

We further investigated whether the East-West Eurasian population differentiation was also present, or even stronger, among woolly rhinoceroses in their nuclear genomes. In contrast to mitochondrial phylogeny (Fig. 2A and fig. S9), the autosomal phylogeny (Fig. 4A), multidimensional scaling plot (Fig. 4B) and outgroup f_3-statistics (fig. S12) among individuals reveal a clear spatiotemporal structure, with individuals from the same regions and periods clustered together (Fig. 4, A and B, and fig. S12). The oldest individual (~170 ka) in our dataset (data S6), QGRH004 (EA_MIS6) from Qinggang, Northeast China, occupied a basal position among all woolly rhinoceroses in the autosomal phylogeny (Fig. 4A) and shared the least genetic affinity with other individuals (fig. S12). The seven Late Pleistocene individuals from East Asia (EA_MIS5-3) and eight non–East Asian individuals formed two different clusters, with the oldest non–East Asian individual, ~102-kyr-old IAER008 (Altai_MIS5) from the Denisova Cave (data S6) ancestral to all younger individuals from the Altai region, East Europe, and Northeast Siberia (Fig. 4A). The European and Altai individuals shared a close genetic affinity (fig. S12), consistent with their similar mitochondrial haplogroup composition (Fig. 2B) and low pairwise F_{ST} (data S11). These findings suggest that the gene pool of woolly rhinoceroses in the Late Pleistocene may have included a substantial contribution from East Asia. The East Asian and non–East Asian populations diverged at least ~102 ka, broadly corresponding to MIS 5. The non–East Asian genetic diversity probably emerged in the Altai region and further spread to Northeast Siberia and Europe.

In contrast to the mitochondrial results (Fig. 2), two Northeast Siberian woolly rhinoceroses (NESIB) share a higher nuclear genetic affinity with West Eurasian individuals than with East Asian individuals (Fig. 4A and fig. S12). However, in the outgroup f_3-statistics, we noticed an extra affinity between these Northeast Siberian and EA_MIS5-3 individuals (fig. S12). The two Last Glacial Maximum (LGM; 26.5 to 19 ka) East European individuals (EE_MIS2) also show extra affinity with contemporaneous Altai individuals (Altai_MIS2) (fig. S12). Therefore, we further applied a series of f_4-statistics to explore whether gene flow among different populations had contributed to the genetic structure of the woolly rhinoceros.

Despite the deep divergence, the EA_MIS6 lineage shares a closer genetic affinity with the local Late Pleistocene (EA_MIS5-3) population, according to f_4(Sumatran, EA_MIS6; EA_MIS5-3, Altai/EE/NESIB pops) [absolute Z-score (|Z|) > 3; data S13]. This suggests potential genetic contributions from other ancestral lineages in the non–East Asian populations. Indeed, the admixture graph modeling of woolly rhinoceros populations also reveals a similar pattern, where both Altai and East European populations received additional gene flow from ghost lineages that were ancestral to the split between EA_MIS6 and Late Pleistocene lineages (Fig. 4D and fig. S13).

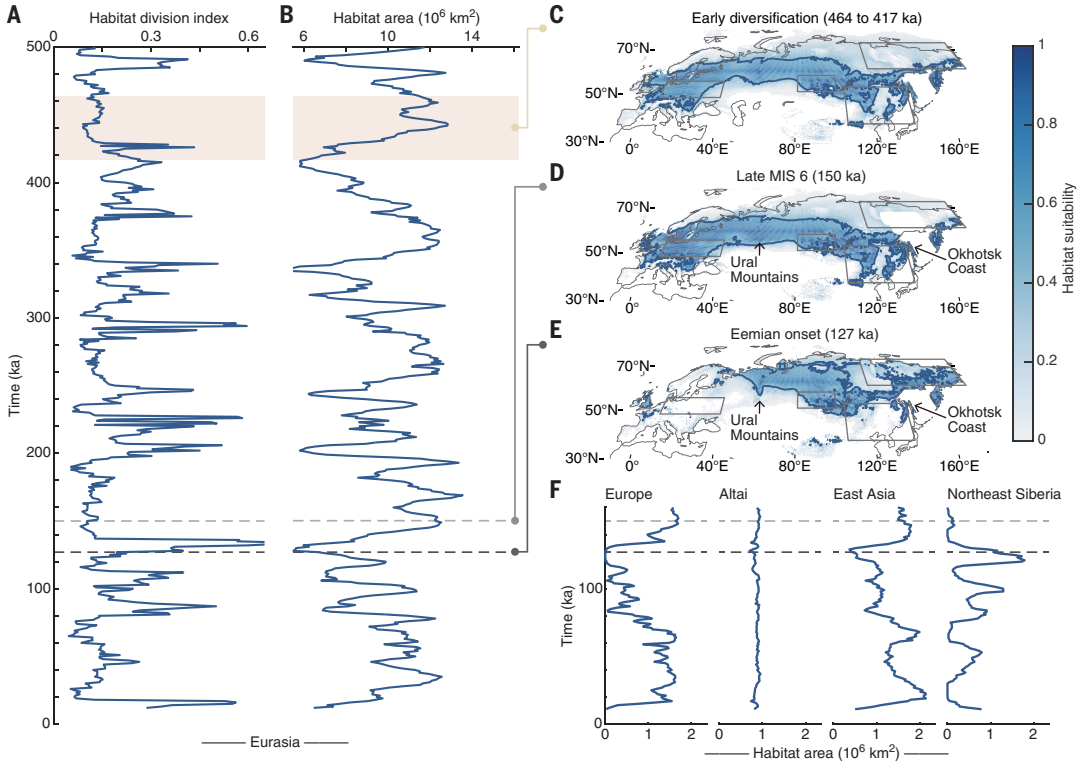

Fig. 3. Spatiotemporal dynamics of woolly rhinoceros habitats. (**A**) Temporal variation in habitat division index (a measure of fragmentation) and (**B**) total suitable habitat area across Eurasia over the past 500 kyr, using a suitability threshold of 0.5. Shading marks the interval overlapping the inferred early lineage divergence. (**C**) Habitat suitability during the early diversification context (464 to 417 ka). (**D** and **E**) Habitat suitability at (D) 150 ka (late MIS 6) and (E) 127 ka (Eemian onset) captures strong late MIS 6–Eemian restructuring in habitat extent and east-west connectivity. (**F**) Regional trajectories of suitable habitat area over the past 160 kyr for Europe, the Altai, East Asia, and Northeast Siberia showing divergent regional responses during the MIS 6–Eemian transition. Boxes in (C) to (E) denote the four regions. Arrows in (D) and (E) indicate the Ural Mountains and the Okhotsk coast. The full spatiotemporal evolution of habitat suitability is shown in movie S1.

The extra affinity between Late Pleistocene East Asian and Northeast Siberian populations was also supported by f_4(Sumatran, EA_MIS5-3; NESIB, Altai/EE pops) (|Z| > 3; data S13), suggesting a high connectivity between East Eurasian populations. Compared with the pre-LGM East European individual (EE_MIS3), the LGM individuals were significantly more closely related to the LGM Altai individuals and Northeast Siberian individuals, according to f_4(Sumatran, Altai_MIS2/NESIB; EE_MIS3, EE_MIS2) (|Z| > 3; data S13). The admixture graph modeling also showed genetic contribution from a NESIB-related lineage in the EE_MIS2 population and the LGM Altai population as the admixture of EE_MIS2, NESIB, and local Altai lineages (Fig. 4D and fig. S13). These analyses reveal increased genetic exchange among different woolly rhinoceros populations across Eurasia during the LGM, especially highlighting gene flow from a high-latitude Northeast Siberian population into mid-latitude regions. This may be best explained by habitat expansion in mid-latitudes, contraction in high latitudes, and greater east-west connectivity as climate cooled toward the start of the LGM (Fig. 3F and fig. S3).

Together, these findings suggest that East Asia was one of the sources of genetic diversity for Late Pleistocene woolly rhinoceroses across Eurasia. The Altai region may have functioned as a reservoir for genetic ancestry before the Late Pleistocene and as an important dispersal hub for woolly rhinoceroses across western and northern Eurasia, which is supported by the persistence of suitable habitats under varying climatic conditions (Fig. 3F). The smaller amount of runs of homozygosity observed in an East Asian individual (fig. S14), along with the significantly higher genomic heterozygosity of East Asian and Altai individuals compared with that of East European and Northeast Siberian individuals, further support both regions as important sources of genetic diversity of the species (Fig. 4C and data S14).

Genetic introgression from Merck's rhinoceros in woolly rhinoceroses

Cross-species gene flow among different extant and extinct lineages could have played an important role in the evolution of rhinoceros species (*13*). The Merck's rhinoceros was the closest surviving relative of the woolly rhinoceros in the Late Pleistocene and largely overlapped with woolly rhinoceroses in their spatiotemporal distribution (*13*). However, owing to their genetic proximity, it remains challenging to test whether gene flow occurred between these two sister lineages.

Using f_4(Sumatran, Merck; WoollyPop1, WoollyPop2) (|Z| > 3; data S13), we detected the greatest shared affinity with the Merck's rhinoceros in woolly rhinoceroses from Northeast Siberia. As the Merck's rhinoceros individual was also from Late Pleistocene Northeast Siberia (*13*), we suggest that the genetic interaction happened locally between the two sympatric species, no later than MIS 3 (the ages of the studied samples). The Late Pleistocene East Asian individuals also showed extra affinity to the Merck's rhinoceros (|Z| > 3; data S13). Considering the broad distribution of Merck's rhinoceroses (*13*, *38*, *39*), especially in East Asia, the shared affinity in these woolly rhinoceroses might be introduced from separate gene flow events with local Merck's rhinoceroses. The individual level f_4-statistics, f_4(Sumatran, Merck; other Ind, EA_MIS5-3 Ind) (|Z| > 3; data S13), further reveal increased affinity to Merck's rhinoceros from MIS 5 to MIS 3. This suggests that the introgression likely started between MIS 6 and MIS 5 and further continued at least until MIS 3.

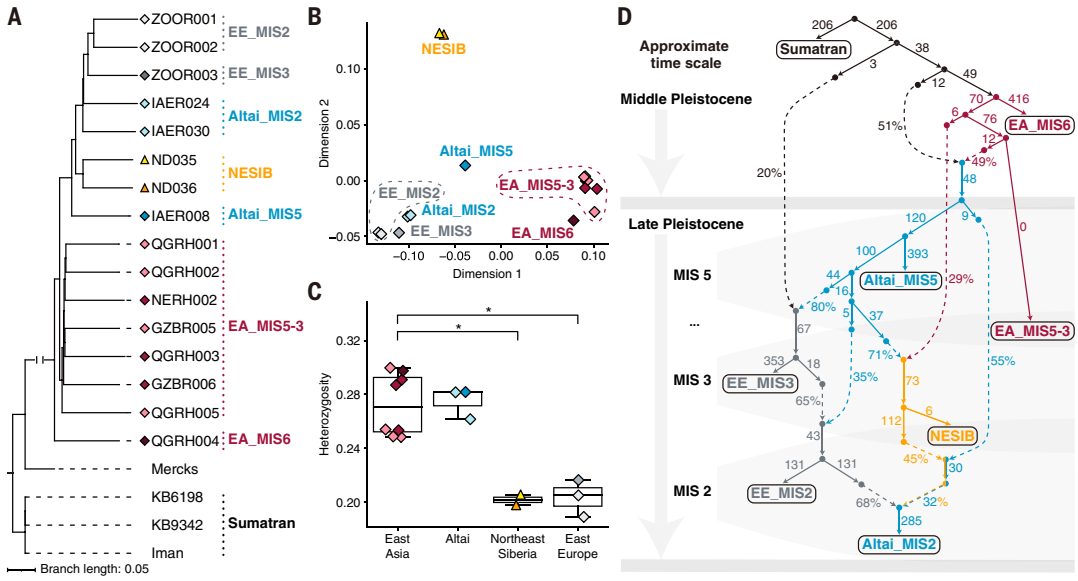

Fig. 4. Nuclear population structure, gene flow, and genetic diversity of woolly rhinoceroses. (**A**) Neighbor-joining phylogeny based on autosomal variants with all nodes supported by 100/100 bootstrap replicates. The color and shape of each sample show the region and age corresponding to Fig. 1, with the sample grouping annotated. (**B**) Multidimensional scaling plot using PLINK. Marker types and group classifications are consistent with (A). (**C**) Population diversity represented by individual heterozygosities across different regions. Marker types are consistent with those shown in (A). Wilcoxon rank-sum tests were used to assess differences in heterozygosity among regions. $*P < 0.05$. (**D**) Admixture graph modeling of woolly rhinoceros populations using qpGraph ($Z = 2.238$). Details of the graph are described in supplementary materials section "Admixture graph modeling."

In addition, the introgression signal was also observed in LGM East European individuals but not in the MIS 3 individual from the same region, suggesting a gene flow event between MIS 3 and MIS 2 ($|Z| > 3$; data S13). However, it was commonly believed that the Merck's rhinoceros went extinct in Europe after the Last Interglacial ~115 ka (*40*) and therefore could not have coexisted and interbred with European woolly rhinoceroses during the LGM. A different scenario to explain this signal would involve gene flow from Northeast Siberian woolly rhinoceroses (Fig. 4D) during the migration of woolly rhinoceroses from higher- to lower-altitude regions during climatic cooling.

Climatic habitat shifts shaped the population structure of the woolly rhinoceros

By integrating large scale ancient genomic analyses with global habitat-suitability modeling, we were able to provide a spatiotemporally detailed picture of woolly rhinoceros populations in the context of Late Quaternary climatic and environmental change. The main habitat-dynamics patterns inferred from the model were robust to repeated site-level leave-out validation and complementary sensitivity analyses (Fig. 3, figs. S5 to S8, and movie S1).

During the Penultimate Glacial Period (191 to 130 ka), the habitats suitable for woolly rhinoceroses were widely distributed across mid-latitude Eurasia (Fig. 3D and movie S1). From the Eemian onset period (130 to 126 ka), suitable habitats vanished in major parts of East Asia and Europe, whereas they were sustained in large parts of central Eurasia, ranging from the Ural to Altai regions (Fig. 3E). Pairwise sequentially Markovian coalescent analyses also revealed a substantial decline in the effective population sizes of woolly rhinoceroses from East Asia, Northeast Siberia, and East Europe (fig. S15), supporting the sizable impact of the Eemian interglacial period (130 to 115 ka) on woolly rhinoceros populations, as shown in previous studies (*11*, *14*). However, the population decline was not as substantial in the Bayesian skyline plot based on mitochondrial genomes, which may suggest a weaker effect on maternal genetic diversity or a limited resolution (fig. S16).

The Altai region remained a suitable habitat at least in the past 160 kyr (Fig. 3F), supporting its role as a refugium for woolly rhinoceroses during the Late Pleistocene climatic oscillations. Altai_MIS5 dated to ~102 ka also appears to have contributed substantially to the major gene pool across Eurasia after the Eemian interglacial. Together, these results support the hypothesis that populations reexpanded from the Altai refugium across Eurasia as east-west habitat connectivity increased during climate cooling after the Eemian interglacial period (Fig. 3B and fig. S7).

Parts of the Russian Far East also remained suitable during the Eemian interglacial period (Fig. 3F and movie S1), indicating that the region may have functioned as another interglacial refugium. A local population may have been preserved there and kept relatively isolated from central Eurasia. This is consistent with the observed deep divergence between East Asian and non–East Asian populations in the Late Pleistocene (Fig. 4A). During the same period, the increase of suitability in high-latitude Siberia (Fig. 3F) may have opened up a passage along the Okhotsk coast (Fig. 3E) that allowed for woolly rhinoceros migration from East Asia to Northeast Siberia. This could also explain the East Asian ancestry detected in the Northeast Siberian population (Fig. 4D and data S13).

Among the studied regions, Europe experienced the most extreme decline of habitat suitability at the Eemian onset period and did not recover until ~70 ka (Fig. 3, E and F). This may explain the low nuclear genetic diversity in the East European woolly rhinoceroses (Fig. 4C). However, the European samples still showed a relatively high mitochondrial diversity (data S12), and genetic contribution from an early derived ghost lineage was found in East European nuclear genomes (Fig. 4D and fig. S13). These findings suggest that the Middle Pleistocene European woolly rhinoceroses might have also survived in a refugium during MIS 5, perhaps around the Ural Mountains, where our distribution modeling indicates more favorable habitats at this time (Fig. 3E and movie S1). This population may have contributed to the later redispersal of woolly rhinoceroses into East Europe. Paleontological studies have also described the Middle Pleistocene

woolly rhinoceroses in Europe as a separate subspecies (*C. a. praecursor*), indicating a potentially deep divergence between the East and West Eurasian populations (*7*). The lack of older genomes from Europe has, however, limited our ability to test these hypotheses. Further genetic study of Middle and early Late Pleistocene woolly rhinoceroses from Europe would be crucial to reconstruct the dynamics of European populations, unveil the early divergence between East and West Eurasian populations, and further resolve the origin of the woolly rhinoceros as a species.

Unlike the woolly mammoth, another cold-adapted Ice Age megafauna species (*17*, *18*), most of the genetic diversity of the woolly rhinoceros emerged in mid-latitude Eurasia instead of high-latitude Northeast Siberia. This is consistent with previous paleontological and paleoecological studies, which revealed a much wider distribution of the woolly rhinoceros in mid-latitude regions and higher ecological tolerance to both cold and temperate environments (fig. S17) when compared with the woolly mammoth (*10*, *23*, *41*). Originating from the Tibetan Plateau, the *Coelodonta* lineage was believed to acquire the cold adaptation in a plateau preadaptation strategy and remained largely restricted to Central and East Asia until ~600 ka, whereas the *Mammuthus* lineage and many Arctic species were already widely present in high-latitude North Asia by the Early Pleistocene (*1*, *4*, *5*). The habitat modeling also suggests that although high-latitude Northeast Siberia remained suitable for woolly rhinoceroses during the warmest periods, southern central Siberia offered more favorable conditions across glacial-interglacial cycles, at least during the past 160 kyr (Fig. 3D and movie S1).

Our findings underscore the importance of expanding ancient DNA studies in mid- and low-latitude regions. This is because even for cold-adapted species, substantial genetic diversity may have originated and persisted at lower latitudes. Although excellent DNA preservation in northern Eurasia has facilitated deep-time genetic studies, this preservation bias toward high-altitude regions may obscure the full scope of population structure and evolutionary history.

REFERENCES AND NOTES

1. R.-D. Kahlke, *Quat. Sci. Rev.* **96**, 32–49 (2014).
2. A. J. Stuart, A. M. Lister, *Quat. Sci. Rev.* **51**, 1–17 (2012).
3. K. Zhao *et al.*, *Acta Anthropol. Sinica* **41**, 551–562 (2022).
4. J. R. Stewart, I. G. Alsos, A. G. Brown, L. Dalén, P. D. Heintzman, *Trends Ecol. Evol.* **40**, 687–698 (2025).
5. T. Deng *et al.*, *Science* **333**, 1285–1288 (2011).
6. A. Borrani *et al.*, *Cladistics* **42**, 46–62 (2026).
7. A. Uzunidis, P.-O. Antoine, J.-P. Brugal, *Quat. Sci. Rev.* **288**, 107594 (2022).
8. R.-D. Kahlke, F. Lacombat, *Quat. Sci. Rev.* **27**, 1951–1961 (2008).
9. Y. Wang *et al.*, *Nature* **600**, 86–92 (2021).
10. D. A. Fordham *et al.*, *Proc. Natl. Acad. Sci. U.S.A.* **121**, e2316419121 (2024).
11. E. Lord *et al.*, *Curr. Biol.* **30**, 3871–3879.e7 (2020).
12. E. D. Lorenzen *et al.*, *Nature* **479**, 359–364 (2011).
13. S. Liu *et al.*, *Cell* **184**, 4874–4885.e16 (2021).
14. S. M. Guðjónsdóttir *et al.*, *Genome Biol. Evol.* **18**, evaf239 (2026).
15. J. Yuan *et al.*, *BMC Ecol. Evol.* **23**, 56 (2023).
16. P. A. Seeber *et al.*, *Biol. Lett.* **19**, 20230343 (2023).
17. J. C. Chacón-Duque *et al.*, *Mol. Biol. Evol.* **42**, msaf065 (2025).
18. T. van der Valk *et al.*, *Nature* **591**, 265–269 (2021).
19. O. Farber, R. Kadmon, *Ecol. Modell.* **160**, 115–130 (2003).
20. J. Ruan *et al.*, *Science* **381**, 699–704 (2023).
21. A. Timmermann *et al.*, *Nature* **604**, 495–501 (2022).
22. E. Zeller *et al.*, *Science* **380**, 604–608 (2023).
23. A. Y. Puzachenko, V. A. Levchenko, F. Bertuch, E. P. Zazovskaya, I. V. Kirillova, *Quat. Sci. Rev.* **263**, 106994 (2021).
24. R. D. Plotz, W. J. Grecian, G. I. H. Kerley, W. L. Linklater, *PLOS ONE* **11**, e0150571 (2016).
25. N. le Roex, C. Dreyer, P. Viljoen, M. Hofmeyr, S. M. Ferreira, *Mamm. Biol.* **99**, 81–87 (2019).
26. A. G. Rowe *et al.*, *Sci. Adv.* **10**, eadk0818 (2024).
27. A. A. Makati *et al.*, *Ecol. Evol.* **15**, e70758 (2025).
28. R. Juma *et al.*, *Ecol. Evol.* **15**, e72197 (2025).
29. D. Chang *et al.*, *Sci. Rep.* **7**, 44585 (2017).
30. R. V. K. Mellya *et al.*, *Conserv. Genet.* **24**, 905–919 (2023).
31. F. Sánchez-Barreiro *et al.*, *Mol. Biol. Evol.* **40**, msad180 (2023).
32. Y. Ishida, N. J. Georgiadis, T. Hondo, A. L. Roca, *Evol. Appl.* **6**, 253–265 (2013).
33. N. J. van Strien, thesis, Wageningen University & Research (1985).
34. A. Laurie, *J. Zool.* **196**, 307–341 (1982).
35. G. Wittemyer, I. Douglas-Hamilton, W. M. Getz, *Anim. Behav.* **69**, 1357–1371 (2005).
36. T. K. Athira, T. N. C. Vidya, *J. Indian Inst. Sci.* **101**, 257–278 (2021).
37. C. M. Brand *et al.*, *PLOS ONE* **15**, e0231832 (2020).
38. Y. V. Lobachev *et al.*, *Palaeontol. Electronica* **24**, a14 (2021).
39. K. Stefaniak *et al.*, *Quat. Int.* **674-675**, 87–108 (2023).
40. K. Stefaniak *et al.*, *N. Jb. Geol. Paläont. Neues Jahrb. Geol. Paläontol. Abh.* **308**, 45–77 (2023).
41. J. Ma *et al.*, *Quat. Int.* **591**, 93–106 (2021).
42. J. Ruan, X.-L. Lei, H. Yu, Code and data for Figure 3: Woolly rhinoceros habitat modelling, v1.0. Zenodo (2026); https://doi.org/10.5281/zenodo.19823247.

ACKNOWLEDGMENTS

We thank the National Center for Protein Sciences at Peking University in Beijing, China, for assistance with the Protein Platform and G. Li and X. Zhang for help with the MGI-2000 next-generation sequencing experiment. We thank Novogene and the Swedish National Genomics Infrastructure at the Science for Life Laboratory for providing the high-throughput sequencing facility. We thank S.-J. Luo for her support in the ancient DNA lab facilities and Y. Zhang from the Natural History Museum of China for granting access to the samples and supporting the exploratory work in this study. We thank X. Liu from the School of Life Sciences, Peking University; Z. Lin from the Quaternary Paleontology Fossil Museum of Qinggang; and D. Liu and R. Zhang from the Natural History Museum of China for their assistance in sample collection. The radiocarbon determinations were provided by the Higham Lab at the University of Vienna, Austria; X. Wu, Y. Gao, and Y. Lin from the School of Archaeology and Museology, Peking University; and Beta Analytic. We thank B. De Cahsan from the Globe Institute, University of Copenhagen; and S. Liu from the Institute of Zoology, Chinese Academy of Sciences, for guidance on the geographic range of the woolly rhinoceros. We thank W. Yu from the School of Life Sciences, Peking University, for laboratory work. The study by S.M. and A.B. was conducted under the state assignment of Lomonosov Moscow State University. The work of S.V. (with Zoological Museum of Moscow University materials) was conducted under the state assignment of Lomonosov Moscow State University. We thank C. Chacón-Duque from the Centre for Palaeogenetics for guidance on runs of homozygosity analyses and for valuable suggestions during the revision of the text. During the preparation of this work, we used ChatGPT for limited language editing and polishing; we manually reviewed the content and take full responsibility for the content of the published article. **Funding:** This work was funded by Swedish Research Council grant 2021-00625 (L.D.), European Union European Research Council (ERC) grant 101054984, PrimiGenomes (L.D.), Russian Science Foundation grant 24-18-00069 (M.K., S.V., M.S.), National Key R&D Program of China grant 2023YFF0905700 (Q.S.), Priority Academic Program Development of Jiangsu Higher Education Institutions (Q.S.), National Natural Science Foundation of China grants U2574201 and 32570732 (H.Y.) and 42488201 (J.R.), and Institute for Basic Science grants IBS-R028-Y3 and IBS-R028-D1 (J.R.). **Author contributions:** Conceptualization: H.Y.; Data curation: X.-L.L., J.R., R.T.; Formal analysis: X.-L.L., J.R.; Funding acquisition: H.Y., L.D., M.K., S.V., M.S., Q.S., J.R.; Investigation: X.-L.L., X.L., R.T., J.Z., A.G., X.Z., Y.H., Q.S.; Methodology: H.Y., X.-L.L., J.R.; Project administration: H.Y., X.-L.L.; Resources: M.K., S.V., S.M., S.K., S.X., T.W., V.B., L.M., B.S., M.S., K.D., A.B.; Supervision: H.Y., L.D.; Validation: H.Y., X.-L.L., J.R.; Visualization: X.-L.L., J.R., Z.Z., H.-Y.Y.; Writing – original draft: H.Y., X.-L.L., J.R.; Writing – review & editing: H.Y., X.-L.L., J.R., and all authors. **Diversity, equity, ethics, and inclusion:** The paleontological specimens investigated in this study were obtained in collaboration with local paleontologists and museum curators. These individuals were also included as coauthors for their contributions to the collection of materials and background information on studied sites. The samples were collected following the standards of paleogenomic research to minimize damage to the specimens. **Competing interests:** The authors declare that they have no competing interests. **Data, code, and materials availability:** The raw sequencing data from Peking University are available at the Genome Sequence Archive (https://ngdc.cncb.ac.cn/gsa/) under project no. PRJCA047504. The assembled mitochondrial genomes have been deposited in GenBank under accession nos. PZ282242 to PZ282270. All code and archived data necessary to reproduce the analyses and generate the component panels of Fig. 3 are available at Zenodo (*42*); the final composite figure was assembled from these panel outputs. Fossil materials are housed at Peking University and research institutes as described in data S1 and supplementary materials section "Provenance," including the Institute of Archeology and Ethnography of the Siberian Branch of the RAS, the Zoological Museum of Lomonosov Moscow State University, Vernadsky State Geological Museum, the Natural History Museum of China, the Quaternary Paleontology Fossil Museum of Qinggang, and the University of Vienna. The materials can be accessed upon request to corresponding author H.Y. or the fossil-access contact person indicated in data S1 and supplementary materials section "Provenance."

SUPPLEMENTARY MATERIALS

science.org/doi/10.1126/science.aed0430
Materials and Methods; Figs. S1 to S17; References (*43–102*); MDAR Reproducibility Checklist; Movie S1; Data S1 to S14

Submitted 3 November 2025; accepted 14 July 2026

10.1126/science.aed0430

Paleogenomics and habitat modeling reveal temperate Eurasian origins of woolly rhinoceroses

, , , Raquel Teixeira, , Alexandre Gilardet, , , , , Maxim Kozlikin, Sergey Vasiliev, Stanislav Medvedev, Sergei Kruskop, , , Vera Basova, , , , Katerina Douka, Michael Shunkov, Alexandra Buzhilova, Love Dalén, and

Science **393** (6816), . DOI: 10.1126/science.aed0430

Editor's summary

As is the case for other Ice Age megafauna, our understanding of the woolly rhinoceros (*Coelodonta antiquitatis*) has been shaped by samples found primarily in extremely cold climates. Lei *et al*. sequenced 29 mitochondrial and 14 autosomal genomes from ancient woolly rhinoceros specimens found across Eurasia. Compared with previous samples from northeast Siberia, the authors found much more genetic diversity in midlatitude Eurasia, particularly East Asia, and detected the presence of gene flow with the extinct Merck's rhinoceros. Climate modeling coupled with these diversity patterns suggested that the Altai region likely served as a refugium during warm periods. These results highlight the importance of extending the search for ancient DNA to more southern climes if we hope to fully understand such extinct species. —Corinne Simonti